JULY 1994

ECN-RX--94-035

ECN
energy innovation

UNCERTAINTY CALCULATIONS MADE EASIER

A. HOGENBIRK

The Netherlands Energy Research Foundation ECN is the leading institute in the Netherlands for energy research. ECN carries out basic and applied research in the fields of nuclear energy, fossil fuels, renewable energy sources, policy studies, environmental aspects of energy supply and the development and application of new materials.

ECN employs more than 900 staff. Contracts are obtained from the government and from national and foreign organizations and industries.

ECN's research results are published in a number of report series, each series serving a different public, from contractors to the international scientific world.

This RX-series is used for publishing pre-prints or reprints of articles that will be or have been published in a journal, or in conference or symposium proceedings.

Please do not refer to this report but use the reference provided on the title page: 'Submitted for publication to ...' or 'Published in ...'.

Het Energieonderzoek Centrum Nederland (ECN) is het centrale instituut voor onderzoek op energiegebied in Nederland. ECN verricht fundamenteel en toegepast onderzoek op het gebied van kernenergie, fossiele-energiedragers, duurzame energie, beleidsstudies, milieuaspecten van de energievoorziening en de ontwikkeling en toepassing van nieuwe materialen.

Bij ECN zijn ruim 900 medewerkers werkzaam. De opdrachten worden verkregen van de overheid en van organisaties en industrieën uit binnen- en buitenland.

De resultaten van het ECN-onderzoek worden neergelegd in diverse rapportenseries, bestemd voor verschillende doelgroepen, van opdrachtgevers tot de internationale wetenschappelijke wereld.

Deze RX-serie wordt gebruikt voor het uitbrengen van pre-prints of reprints van artikelen die in een tijdschrift of in proceedings van conferenties of symposia (in definitieve vorm) zullen verschijnen of al zijn verschenen.

Gelieve niet te refereren aan het rapportnummer, maar de verwijzing te gebruiken die hiernaast op de titelpagina figureert: 'Voor publikatie aangeboden aan ...' of 'Verschenen in ...'.

Netherlands Energy Research Foundation ECN
P.O. Box 1
NL-1755 ZG Petten
the Netherlands
Telephone : +31 2246 49 49
Fax : +31 2246 44 80

This report is available on remittance of Dfl. 35 to:
ECN, General Services,
Petten, the Netherlands
Postbank account No. 3977703.
Please quote the report number.

Energieonderzoek Centrum Nederland
Postbus 1
1755 ZG Petten
Telefoon : (02246) 49 49
Fax : (02246) 44 80

Dit rapport is te verkrijgen door het overmaken van f 35,-- op girorekening 3977703 ten name van:
ECN, Algemene Diensten
te Petten
onder vermelding van het rapportnummer.

JULY 1994

ECN-RX--94-035

UNCERTAINTY CALCULATIONS MADE EASIER

A. HOGENBIRK

CONTRIBUTION TO 8TH INTERNATIONAL CONFERENCE ON RADIATION SHIELDING
APRIL 24-28, 1994, ARLINGTON, TEXAS

Contribution to
8th International Conference on RADIATION SHIELDING
April 24-28, 1994, Arlington, Texas

UNCERTAINTY CALCULATIONS MADE EASIER

Alfred Hogenbirk
Netherlands Energy Research Foundation ECN
P.O. Box 1
1755 ZG Petten
The Netherlands
tel. (+31) 2246 4051

ABSTRACT

In this paper the results are presented of a neutron cross section sensitivity/uncertainty analysis performed in a complicated 2D model of the NET shielding blanket design inside the ITER torus design, surrounded by the cryostat/biological shield as planned for ITER. The calculations were performed with a code system developed at ECN Petten, with which sensitivity/uncertainty calculations become relatively simple.

In order to check the deterministic neutron transport calculations (performed with DORT), calculations were also performed with the Monte Carlo code MCNP. Care was taken to model the 2.0 cm wide gaps between two blanket segments, as the neutron flux behind the vacuum vessel is largely determined by neutrons streaming through these gaps. The resulting neutron flux spectra are in excellent agreement up to the end of the cryostat. It is noted, that at this position the attenuation of the neutron flux is about 11 orders of magnitude.

The uncertainty in the energy integrated flux at the beginning of the vacuum vessel and at the beginning of the cryostat was determined in the calculations. The uncertainty appears to be strongly dependent on the exact geometry: if the gaps are filled with stainless steel, the neutron spectrum changes strongly, which results in an uncertainty of 70% in the energy integrated flux at the beginning of the cryostat in the no-gap-geometry, compared to an uncertainty of only 5% in the gap-geometry. Therefore, it is essential to take into account the exact geometry in sensitivity/uncertainty calculations.

Furthermore, this study shows that an improvement of the covaraince data is urgently needed in order to obtain reliable estimates of the uncertainties in response parameters in neutron transport calculations.

1 INTRODUCTION

In the design of a next-step fusion device, like ITER, it is of vital importance that uncertainties may be attached to parameters determined in shielding calculations. Therefore, in the framework of the European Fusion File (EFF) project much attention was given in the last few years to sensitivity and uncertainty calculations. This resulted at ECN Petten in the development of a code system (mainly consisting of adjusted existing codes), with which it is possible to determine sensitivities and uncertainties for response parameters in 2-dimensional (2D) shielding calculations. The 2D sensitivity and uncertainty code SUSD [1] plays a main role in this code system.

A major achievement is the use of uncertainty data (more generally, covariance data) for angular- and energy distributions. Processing of these data from basic nuclear data (section MF34 and MF35 of the evaluated nuclear data file (ENDF), respectively) is possible with the cross section processing code NJOY [2] using modules from the modified SUSD code package.

Uncertainty data for angular- and energy distributions (SAD- and SED data, respectively) are usually not present on even the most recent releases of evaluated nuclear data files, such as ENDF/B-VI, EFF-2 and JENDL-3. The European EFF-2 evaluation is an exception, however, as for the main structural materials (Fe, Cr and Ni) uncertainty data for angular distributions were evaluated for energies $E_n > 0.8$ MeV.

In order to show the usefulness of sensitivity/uncertainty calculations for realistic designs, in this paper results are presented of calculations performed for two different shielding designs for a next-step fusion reactor:

- an elaborate design, in which gaps between adjacent blanket segments of the fusion reactor were taken into account ("gap-geometry")
- the same design, in which the gaps were filled with stainless steel ("no-gap-geometry").

It appears, that the uncertainty in relevant response parameters is strongly dependent on the exact geometry and may be as large as 70% (no-gap-geometry) or as small as 5% (gap-geometry) for the same parameter. A significant contribution will be due to uncertainties in angular- and energy distributions of scattered neutrons. Data needed for the latter type

of analysis are still lacking for most elements in nearly all evaluations. However, they are urgently needed for accurate analyses.

2 COMPUTATIONAL DETAILS

2.1 Theoretical basis

The basic theory of sensitivity and uncertainty calculations can be found in the literature [3–5]. Only those quantities needed for the work presented in this paper are touched upon in this section.

First of all the response parameter R should be defined, which is a function of the neutron flux ϕ_n at a certain position. Interesting response parameters may be the energy integrated flux, the nuclear heating or the nuclear damage.

Once the response parameter has been defined, it should be used as a neutron source in an adjoint neutron transport calculation. Forward and adjoint angular fluxes can then be used to compute sensitivities and uncertainties.

A good insight in which cross sections at which energies play an important part in the sensitivity of a specific response parameter is obtained by a comparison of *sensitivity profiles* for different cross sections.

A sensitivity profile $P^g_{\Sigma_i}$ for a given response parameter R and cross section Σ_i is defined as [6]

$$P^g_{\Sigma_i} = \frac{\delta R}{R} / \frac{\delta \Sigma^g_i}{\Sigma^g_i} \qquad (1)$$

with g the neutron energy group index. Thus, $P^g_{\Sigma_i}$ indicates the relative change in a response parameter R due to a relative change in Σ_i at energy E_g.

A useful quantity is the *integrated sensitivity* S_{Σ_i}, defined as

$$S_{\Sigma_i} = \sum_g P^g_{\Sigma_i}. \qquad (2)$$

The integrated sensitivity can be interpreted as the fractional change of a response parameter R as a result of a fractional change of cross section Σ_i in *all* energy groups.

Final uncertainties are determined by the magnitude of the sensitivity profiles as well as by the values of the covariance matrix elements. It can be derived (see [6]), that the relation between the sensitivity profile $P^g_{\Sigma_i}$ and the resulting relative uncertainty $\frac{\Delta R}{R}$ is given by

$$\left(\frac{\Delta R}{R}\right)^2 = \sum_i \sum_j \sum_g \sum_{g'} P^g_{\Sigma_i} P^{g'}_{\Sigma_j} \frac{Cov(\Sigma^g_i, \Sigma^{g'}_j)}{\Sigma^g_i \Sigma^{g'}_j} \qquad (3)$$

Covariance matrices may be found on the evaluated data files. For this work a processed library was used (ZZ-VITAMIN-J/COVA), which was obtained from the NEA Data Bank.

2.2 Code system

An outline of the code system used in this analysis is given in fig. 1. The 2D sensitivity/uncertainty code SUSD [1,7] plays a central role in this system. It is noted, that several modules of the cross section processing code NJOY [2] and two modules of the SUSD-package (i.e. GROUPSR and SEADR) are needed in order to produce libraries for use in SUSD. Neutron transport calculations may be performed with standard codes (ANISN [8] or ONEDANT [9] for 1D calculations, DORT [10] or TWODANT [11] for 2D calculations).

The code system shown in fig. 1 was developed at ECN Petten. It mainly consists of existing codes, which were adjusted in order to enable a good communication between the codes. Especially large modifications were applied to SUSD, SEADR and GROUPSR.

The code SUSD is probably the most sophisticated sensitivity/uncertainty code to date. Various kinds of cross section sensitivities/uncertainties can be treated. Moreover, a calculation is possible of uncertainties due to uncertainties in energy- and angular distributions of scattered neutrons (SED- and SAD-uncertainties, respectively). The contribution of the latter kind of uncertainties to the uncertainty in a response parameter may be large, but only very few codes exist which can treat SED/SAD-uncertainties.

3 SAMPLE CASE

As an interesting sample case a complete sensitivity/uncertainty analysis was performed for a 2D model of the NET shielding-blanket design inside the ITER torus-design, surrounded by the cryostat/biological shield as planned for ITER. In this specific geometry a difficulty is present, as the outboard blanket segments are separated by gaps with a width of 2.0 cm. This implies, that for neutron transport calculations the gap region has to be taken into account very accurately, as most of the radiation transport will take place through these gaps. A schematic diagram of the geometry is given in fig. 2.

In order to study the effect of the presence of these gaps on radiation levels outside the torus, neutron transport calculations were performed for two closely related geometries:

- one in which the gaps are present ("gap-geometry")
- one in which the gaps are filled with stainless steel ("no-gap-geometry").

Sensitivity/uncertainty calculations were performed for both geometries, using the code system described in section 2. Response parameters were taken to be the energy-integrated neutron flux at the beginning of the vacuum vessel (important for the welds of the vacuum vessel) and at the beginning of the cryostat (important for the dose rate outside the reactor).

3.1 Geometry

Only a concise description of the geometry is given in this section. More details can be found in [12]. According to the drawings obtained from the NET-team, the shielding-blanket geometry consists of toroidal stainless steel sections with incorporated cooling-channels.

The gap and the blanket section nearest to the gap were modelled as accurately as possible, correctly representing the

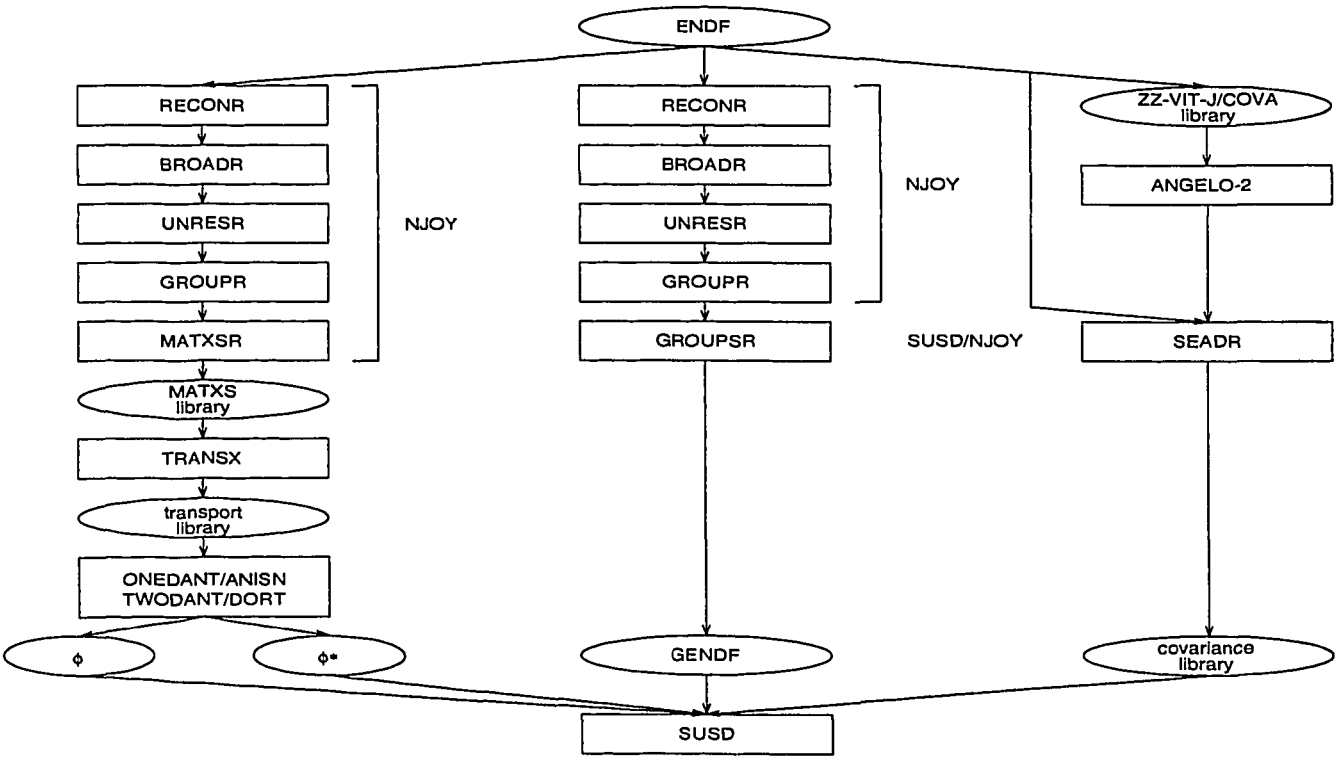

Figure 1: Code system used for the sensitivity and uncertainty calculations.

cooling-channels. The remaining blanket sections containing steel and cooling-water were homogenised into "onion-skin"-wise material-zones.

The backplate was modelled in an analogous way. The second section, which consists of vertical cooling pipes surrounded by steel pebbles, was homogenised.

A simple "onion-skin" type model of the inboard blanket/first wall was included in order to obtain the correct backscatter contribution from the inboard region.

The ITER design of the vacuum-vessel is a complicated structure with a large number of penetrations. In this shielding problem, the vacuum vessel was approximated by a simple "onion-skin" type geometry.

The TF-coils are not of interest for this study, thus they were removed from our model. With respect to the biological shielding this is an acceptable conservative approximation.

The cryostat/biological shield is, apart from the penetrations, a simple geometry consisting of a concrete wall lined at the inside with a steel layer of 6 mm thickness. The main function of the cryostat as a shield will be to reduce the γ-dose rate outside the cryostat after shut-down. The thickness chosen in our model (170 cm) is based on preliminary MCNP calculations.

As a simple "onion-skin" type model for the vacuum vessel is used, the toroidal symmetry of our model is determined by the 48 outer blanket-segments. Thus the model could be restricted to half a blanket segment, spanning a toroidal interval of 3.75°, which is $1/96^{th}$ part of the torus, see fig. 2.

The 14 MeV neutron-source distribution of the plasma was represented by an isotropic volume source at $r = 611 - 620$ cm, resulting in an average neutron wall loading of 1 MW/m^2.

4 2D DETERMINISTIC CALCULATIONS WITH DORT

2D deterministic neutron transport calculations were performed using the code DORT. This code was chosen as it has the provision to use biased quadratures, which are indispensable in this study. For details see [12].

4.1 Spatial and angular discretisation

A detailed spatial- and angular- discretisation was determined in order to guarantee sufficient accuracy for the radiation leakage through the gaps and the deep penetration through the blanket, vessel and cryostat/shield. In the 2D-calculations with DORT the torus was modelled in (r, θ) geometry. Therefore, the cooling-pipes in the first blanket-section (i.e. nearest to the segment-gap) could not be modelled exactly. The spatial mesh was defined in such a way, that each cooling-pipe is enclosed by a spatial (r, θ) mesh, in which the amount of water and steel was homogenised.

The number of the radial mesh-intervals, required to obtain the correct radial flux-attenuation, was determined by performing test calculations with the one-dimensional transport code ANISN [8] in a 1D representation of the torus and

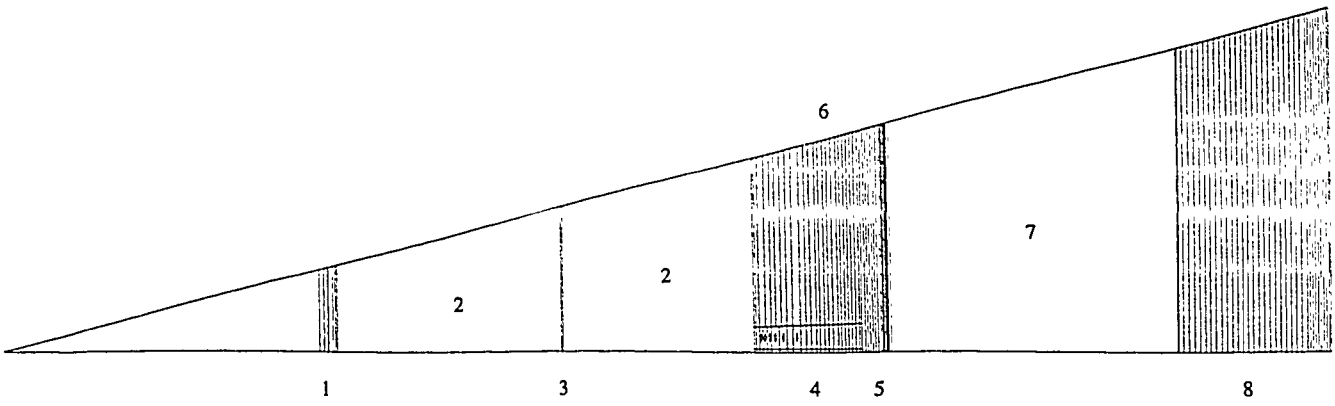

Figure 2: 2D geometrical model used for the description of the NET/ITER torus/vacuum vessel/cryostat/biological shield. The picture is distorted in order to show more detail in the toroidal direction. The planes shown are used in the MCNP calculations as splitting planes, and do not necessarily define material zones. The inboard blanket is indicated by 1, the plasma region by 2, the neutron source by 3, the gap by 4, the vacuum vessel by 5, the outboard blanket by 6, the region between vacuum vessel and cryostat by 7 and the cryostat by 8.

cryostat, in which the number of mesh-intervals was gradually increased. In the final calculations radial mesh-intervals of 2 to 3 cm were used for the material zones and intervals of 20 cm or smaller were used for the plasma- and void- regions.

Toroidally the geometry was subdivided in 11 mesh-intervals ($\tau = \tau_1$ to $\tau = \tau_{11}$). The first interval exactly spans the segment-gap. The adjacent blanket section was subdivided in three intervals. The next 6 toroidal intervals each span one blanket section (with a width of approximately 6 cm), whereas the last toroidal interval spans the 8th and half of the 9th blanket section.

In order to calculate the radiation-leakage through the gaps, a biased angular-quadrature set is required which is biased towards the (r, z) plane to ensure a sufficient number of discrete directions passing through the gaps. A symmetric S_8 quadrature set was used as a starting point. The biased quadrature set was obtained by replacing at each η_j-level (η_j is the direction-cosine with respect to the Z-axis at level j where $j = 1, n/2$) the discrete direction of the S_n set nearest to the (r, z) plane by $NL(> 1)$ new directions. These were distributed quadratically over the azimuthal angle α, such that the distribution is denser towards the (r, z) plane ($\cos\alpha = \mu/\sqrt{1-\eta^2}$, where μ is the direction-cosine with respect to the r-axis.) The weights of these new directions were determined in such a way, that for the resulting biased set the diffusion condition still holds.

In order to determine the value of NL required to treat the gaps in sufficient detail, several biased sets for increasing values of NL were produced. The calculated attenuation over the gap converged at $NL \approx 27$. Therefore in the calculations a biased set was used with 464 directions instead of the 160 directions for the symmetric S_8 quadrature set.

4.2 Cross section data

The group-constants used in the S_n-calculations were derived from the MAT175 (JEF/EFF-1) library [13] (which is in the 175 group VITAMIN-J group-structure), using the processing-code TRAMIX [14] for mixing, collapsing and self-shielding. A library in a 33 group structure was used, which appears to give a good agreement with a library in the 100 group GAM-II structure in a simplified 1D geometry.

It is known from previous studies that in order to describe neutron deep penetration correctly it is essential to take self-shielding explicitly into account. Therefore, self-shielded cross sections were used for all mixtures used in this study.

4.3 Adjoint neutron transport calculations

Adjoint neutron transport calculations were performed with DORT for both response parameters in both the gap-geometry and the no-gap-geometry. The code was used in the forward mode, using adjoint libraries produced by TRAMIX.

5 2D MONTE CARLO CALCULATIONS WITH MCNP

5.1 Geometrical model

In order to check the results from the deterministic calculations 2D Monte Carlo neutron transport calculations were performed as well, using MCNP4 [15].

An accurate estimate of the number of neutrons passing through the gaps is required for a reliable calculation of the response parameters. Therefore, a Monte Carlo calculation without biasing neutrons into the direction of the gaps and, in the gaps, into the direction of the cryostat, is not adequate.

As it is required that a large number of neutrons start from the gap region of the surface of the outboard first wall, we chose to subdivide the complete geometry, as given in fig. 2, in three separate regions:

I the segment gap region,

II the neighbouring blanket-slab region (in this region the water-cooling tubes are modelled explicitly),

III the remaining blanket region.

Using this approach, in the first step of the calculations surface sources were produced on the outboard first wall for each of these three regions using the SSW-card in MCNP.

The remaining calculations were devoted to the transport of neutrons from the surface sources to the outside of the cryostat/biological shield. The weight-window technique was used in order to bias particles into the direction of the segment gap and also into the direction of the cryostat. The splitting planes were chosen in such a way, that a reasonably flat track distribution was obtained [16].

In the cryostat the neutrons were biased radially outward using the exponential transform in MCNP (see [16]) with $p = 0.7$.

On a series of locations response parameters were calculated (fluxes, dose rates, heating). The energy group structure for representing the flux spectra was taken to be identical to the one used in the DORT calculations (see section 4).

5.2 Cross section data

Cross sections were taken from the EFF-1.3 library [17], which is based on the basic nuclear data from the JEF/EFF-1 evaluation. Thus, the cross section data used in these Monte Carlo calculations are consistent with those used in the DORT calculations, which are also based on the JEF/EFF-1 evaluation.

6 SENSITIVITY CALCULATIONS

The sensitivity calculations were restricted to the main consistuents of stainless steel, i.e. Fe, Cr and Ni, as it is known from previous studies that they will be the main contribution to the total uncertainty.

Libraries for use in SUSD were produced for these elements in the 33 group structure. Using NJOY-modules RECONR, BROADR, UNRESR and GROUPR and SUSD module GROUPSR the required GENDF library (see fig. 1) was produced.

The covariance library was obtained from the ZZ-VITAMIN-J/COVA library using the code ANGELO-2 [18] and SUSD-module SEADR. Uncertainty data for the elastic angular distribution (SAD uncertainties) were taken from the EFF-2 evaluation, converted to the SUSD-format by NJOY-module ETSR and added to the covariance library (module ETSR is part of the ECN code package, which will be sent to the NEA Data Bank soon). SAD uncertainty data are only evaluated for energies $E_n > 0.8$ MeV. The uncertainty for energies $E_n < 0.8$ MeV was taken to be equal to the uncertainty at $E_n = 0.8$ MeV. The SAD data are only available in the EFF-2 evaluation and are only given for the elastic cross sections of Fe, Cr and Ni.

Thus, with these libraries as well cross section sensitivity/uncertainty studies can be performed as SAD sensitivity/uncertainty calculations, in which the uncertainty in the angular distribution of the scattered neutrons is taken into account.

Unfortunately, uncertainty data for the energy distribution of scattered neutrons (SED data) are still lacking in the evaluations.

7 RESULTS

7.1 Neutron transport calculations

7.1.1 Comparison DORT - MCNP

As can be seen from the energy-integrated τ-averaged radial neutron flux profile $\phi_{n,av}(r)$ given in fig. 3, there is a good agreement between the results of the deterministic calculations and the results of the Monte Carlo calculations, despite the large attenuation of more than 11 orders of magnitude between the neutron source and the end of the cryostat.

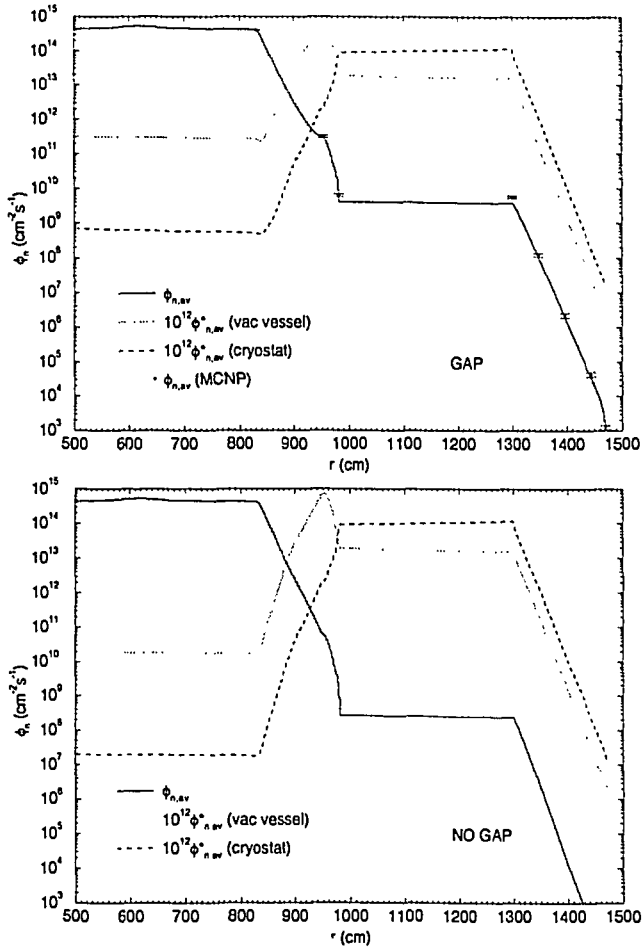

Figure 3: τ-averaged radial flux profiles for the geometry with gaps (above) and without gaps (below). In the upper figure the results of MCNP calculations are also given. Adjoint radial flux profiles for two different responses (energy integrated flux at beginning of vacuum vessel (vac vessel) and energy integrated flux at beginning of cryostat (cryostat)) are given in this figure as well.

A detailed comparison requires that neutron flux *spectra* are compared. An example is given in fig. 4, where neutron spectra calculated by DORT and MCNP at $r = 981.5$ cm (end of vacuum vessel) are shown. It is clear from this figure

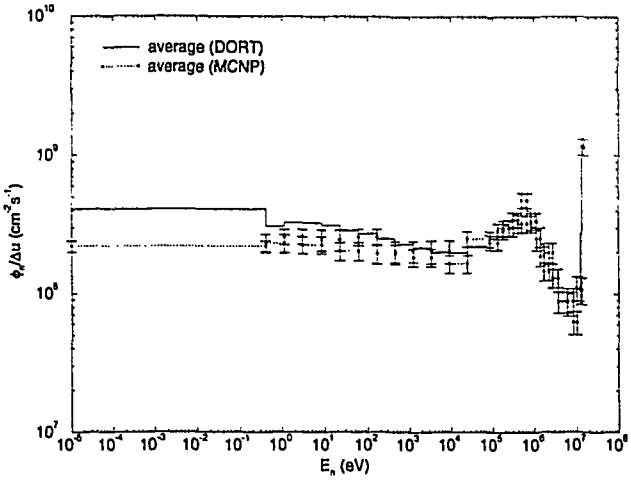

Figure 4: τ-averaged neutron flux spectrum for the gap-geometry at r = 981.5 cm (end of vacuum vessel) as calculated by MCNP and DORT.

that also the calculated flux spectra agree well. An extensive comparison and discussion of the results can be found in [12].

The comparison of the DORT- and MCNP-results shows that consistent results can be obtained for gap streaming problems, provided that the gap region is accurately taken into account.

Therefore, for a comparison of the results for the gap-geometry with those for the no-gap-geometry it is sufficient to take only into account the DORT results.

7.1.2 Comparison of gap-geometry with no-gap-geometry

Results of neutron transport calculations for the gap-geometry and the no-gap-geometry are given in fig. 3.

The effect of the gaps is very clear from this figure: radiation levels are increased by a factor of more than 10 (at the end of the vacuum vessel) to more than 100 (at the end of the cryostat) compared to the situation without gaps.

Neutron spectra calculated by DORT at several locations are given in fig. 5. The spectrum at the first wall is hardly influenced by the presence of the gaps. Therefore, the τ-averaged neutron spectrum in the no-gap geometry (not given in this figure for clarity) nearly coincides with the τ-averaged neutron spectrum in the gap-geometry.

The anisotropy of the toroidal distribution at the beginning of the vacuum vessel is evident, causing the strongly increased flux $\phi_{n,av}$ as observed in fig. 3. The τ-averaged flux (especially at $E_n \gtrsim 1$ MeV) is largely determined by neutrons from the gap region.

No pronounced anisotropy is present in the neutron spectrum at the beginning of the cryostat. Both the radiation level and the neutron spectrum are strongly determined by neutrons travelling through the gaps.

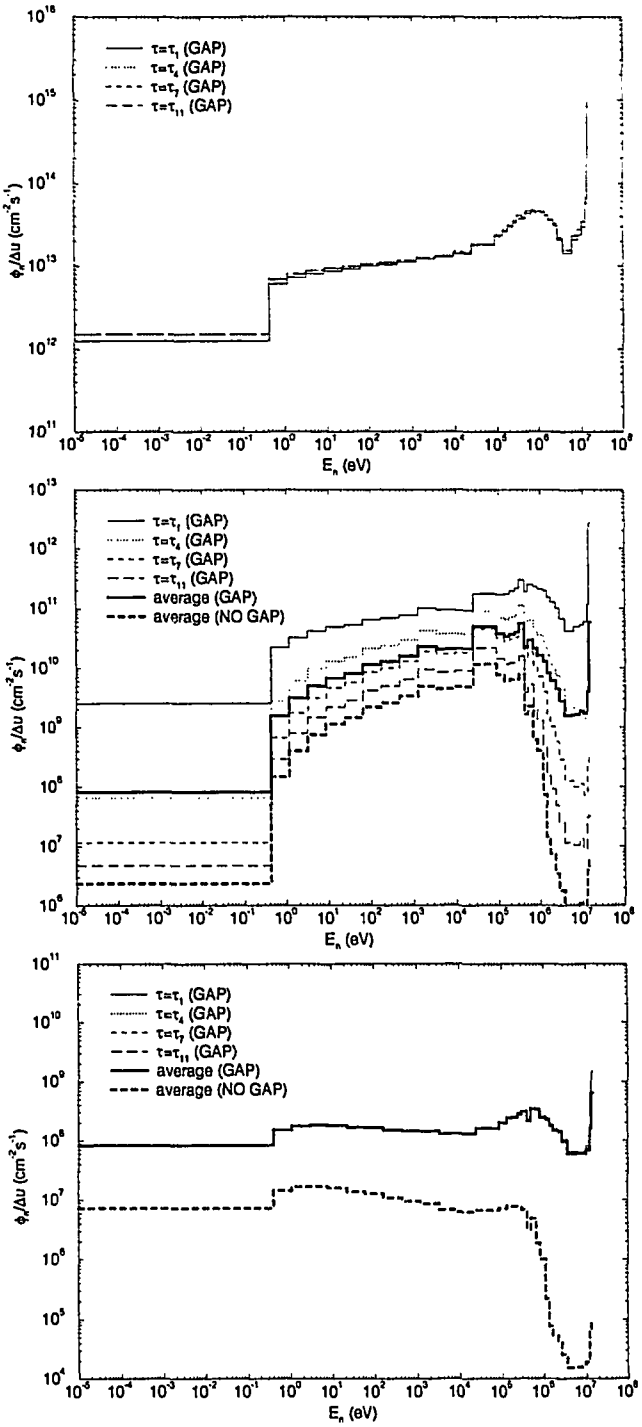

Figure 5: Toroidal flux spectra at the outboard first wall (upper figure), at the beginning of the vacuum vessel (middle figure) and at the beginning of the cryostat (lower figure). Spectra are given for $\tau = \tau_1, \tau_4, \tau_7$ and τ_{11}. In the latter two figs. for comparison the τ-averaged neutron flux spectrum in the geometry with gaps is given as well as the average neutron flux spectrum in the geometry without gaps.

7.2 Sensitivity/uncertainty calculations

As mentioned in section 3 sensitivity/uncertainty calculations were performed for two different response parameters: the

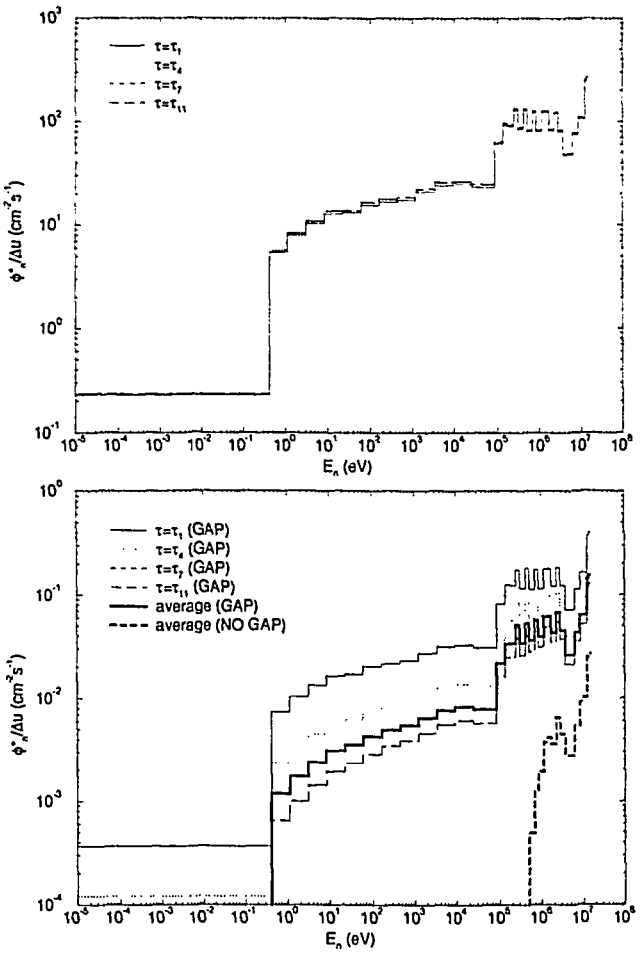

Figure 6: Toroidal adjoint flux spectra at the beginning of the vacuum vessel (upper figure) and at the position of the neutron source ($r = 611 - 620$ cm) (lower figure). Spectra are given for $\tau = \tau_1, \tau_4, \tau_7$ and τ_{11}. In the lower figure for comparison the τ-averaged neutron flux spectrum in the gap- and the no-gap-geometry is given as well. Response parameter: energy-integrated neutron flux at the beginning of the vacuum vessel.

energy-integrated neutron flux at the beginning of the vacuum vessel and the energy-integrated neutron flux at the beginning of the cryostat.

7.2.1 Adjoint neutron transport calculations

Energy-integrated τ-averaged neutron adjoint fluxes are given in fig. 3 for the gap- and the no-gap-geometry, respectively. As expected, the average importance of neutrons from the blanket region is much larger in the gap-geometry, leading to a difference of a factor of more than 10 in the plasma region.

This difference is obvious from a comparison of adjoint flux spectra at the position of the neutron source ($r = 611 - 620$ cm) for both geometries. It is seen from fig. 6 that when gaps are present, neutrons with a broad energy spectrum have a possibility of reaching the vacuum vessel or the cryostat. However, if these gaps are absent, only the most energetic neutrons will succeed in penetrating the blanket.

7.2.2 Sensitivity calculations

This difference is reflected in the sensitivity profiles P_Σ^g (NO GAP) (for the no-gap-geometry) and P_Σ^g (GAP) (for the gap-geometry), given in fig. 7 for the total, elastic and nonelastic cross sections of Fe. Similar profiles were calculated for Cr and Ni. There is a relative increase in P_Σ^g in the $E_n \gtrsim 1$ MeV region for the geometry without gaps. Furthermore, the absolute value of P_Σ^g (NO GAP) is much larger than the absolute value of P_Σ^g (GAP). This reflects the fact, that in the geometry without gaps neutrons suffer far more collisions than in the geometry with gaps.

Resulting integrated sensitivities S for Fe, Cr and Ni cross sections are given in table 1. From this table it is clear, that both the elastic and the nonelastic cross section contribute substantially to the total sensitivity. There is a strong dependence of the neutron energy spectrum, as can be observed for Ni in the no-gap-geometry.

7.2.3 SAD sensitivities

The SAD sensitivity profile for the $l = 1$ component of the elastic cross section of Fe is given in fig. 7 as well. As the anisotropy of the elastic cross section increases with increasing energy, this is reflected in the sensitivity profiles. Again, the sensitivity for the no-gap-geometry is much larger than for the gap-geometry.

7.3 Uncertainty calculations

Sensitivity profiles calculated in section 7.2 were used in order to calculate uncertainties in response parameters. Resulting uncertainties are summarized in table 2. From this table it can be deduced, that if the Fe, Cr and Ni cross sections are supposed to be non-correlated, the final uncertainty in the energy-integrated flux at the beginning of the vacuum vessel amounts to 33% in the no-gap-geometry and 6.5% in the gap-geometry. The uncertainty in energy-integrated flux at the beginning of the cryostat amounts to 72% in the no-gap-geometry and 5% in the gap-geometry. Therefore, there is a huge difference between the uncertainties in both geometries. This implies, that for sensitivity/uncertainty calculations the real geometry has to be taken into account very accurately. The large difference in this case is clearly due to the neutron spectrum which differs strongly between both geometries. Thus, different parts of the covariance matrix become important.

This is evident from the uncertainty in the energy integrated flux at the beginning of the cryostat due to Ni cross sections in the no-gap-geometry. Because of the large uncertainty in the Ni non-elastic cross section at low energies, this uncertainty strongly increases.

Furthermore, it is shown that the importance of SAD uncertainties may be large (especially for Fe), so that they not be neglected.

Table 1: Calculated integrated sensitivities for both response parameters in the gap- and no-gap-geometry. Results for the energy integrated flux at the beginning of the vacuum vessel are given in the upper part of the table. In the lower part of the table the results for the energy integrated flux at the beginning of the cryostat are given.

	Fe				Cr				Ni			
	S_{tot}	S_{SAD}	S_{elas}	S_{nonel}	S_{tot}	S_{SAD}	S_{elas}	S_{nonel}	S_{tot}	S_{SAD}	S_{elas}	S_{nonel}
GAP	-1.22	0.183	-0.694	-0.526	-0.329	0.052	-0.223	-0.106	-0.298	0.029	-0.192	-0.106
NO GAP	-5.85	1.09	-3.50	-2.35	-1.58	0.309	-1.11	-0.473	-1.29	0.179	-0.904	-0.386
GAP	-1.20	0.136	-0.613	-0.587	-0.311	0.038	-0.168	-0.143	-0.296	0.021	-0.164	-0.132
NO GAP	-8.41	1.41	-5.16	-3.25	-2.21	0.392	-1.51	-0.698	-13.2	0.249	-4.87	-8.35

Table 2: Calculated uncertainties for both response parameters in the gap- and no-gap-geometry. Results for the energy integrated flux at the beginning of the vacuum vessel are given in the upper part of the table. In the lower part of the table the results for the energy integrated flux at the beginning of the cryostat are given.

	Fe			Cr			Ni			Sum
	$(\frac{\Delta R}{R})_{tot}$	$(\frac{\Delta R}{R})_{SAD}$	$(\frac{\Delta R}{R})_{elas}$	$(\frac{\Delta R}{R})_{tot}$	$(\frac{\Delta R}{R})_{SAD}$	$(\frac{\Delta R}{R})_{elas}$	$(\frac{\Delta R}{R})_{tot}$	$(\frac{\Delta R}{R})_{SAD}$	$(\frac{\Delta R}{R})_{elas}$	
GAP	1.78%	5.41%	1.00%	2.71%	1.49%	2.22%	0.862%	0.300%	0.781%	6.54%
NO GAP	9.11%	28.1%	5.27%	11.7%	7.75%	10.5%	3.78%	1.57%	3.76%	33.0%
GAP	2.03%	4.37%	0.961%	1.87%	1.20%	1.56%	0.874%	0.236%	0.584%	5.38%
NO GAP	13.3%	42.0%	8.14%	14.3%	11.4%	13.3%	53.4%	2.80%	22.9%	71.7%

8 CONCLUSIONS

- Using the sensitivity/uncertainty code system developed at ECN Petten it is relatively easy to perform sensitivity and uncertainty calculations for elaborate 2D geometries.
- In this paper the results are presented of calculations performed for two designs of shielding blankets for a demo-type fusion reactor (the "gap-geometry" and the "no-gap-geometry"). It appears, that the uncertainty in energy integrated fluxes strongly depends on the neutron spectrum, which is strongly dependent on the exact geometry of the reactor. The uncertainty for the same response parameter may be as large as 70% (no-gap-geometry) or as small as 5% (gap-geometry).
- The contribution of uncertainties in the *angular* distributions of scattered neutrons to the total uncertainty is large. The contribution of uncertainties in the *energy* distributions of scattered neutrons may be large as well. However, data for both types of uncertainties are generally scarce (or even unavailable) in current evaluated nuclear data files.
- The calculated uncertainties may be rather large and should clearly be reduced. It is likely, that the actual uncertainty is smaller than the one calculated. Therefore, there is a clear need for *better* cross section covariance data as well as covariance data for angular- and energy distributions if accurate sensitivity and uncertainty calculations are required.

REFERENCES

[1] K. Furuta, Y. Oka and S. Kondo: *SUSD: A computer Code for Cross Section Sensitivity and Uncertainty Analysis Including Secondary Neutron Energy and Angular Distributions*, Report UTNL-R0185, Nucl. Eng. Res. Lab. University of Tokyo, 1986, NEA Data Bank 1151 package

[2] D. W. Muir and R. E. MacFarlane: *The NJOY Nuclear Data Processing System*, Report LA-9303-M, Los Alamos National Laboratory, 1987

[3] S. A. W. Gerstl and W. M. Stacey Jr.: *A Class of Second-Order Approximate Formulations of Deep Penetration Radiation Transport Problems*, Nucl. Sci. Eng. 51 (1973) 339

[4] D. E. Bartine, E. M. Oblow and F. R. Mynatt: *Radiation-Transport Cross-Section Sensitivity Analysis – A General Approach Illustrated for a Thermonuclear Source in Air*, Nucl. Sci. Eng. 55 (1974) 147

[5] S. A. W. Gerstl, D. J. Dudziak and D. W. Muir: *Cross-Section Sensitivity and Uncertainty Analysis with Application to a Fusion Reactor*, Nucl. Sci. Eng. 62 (1977) 137

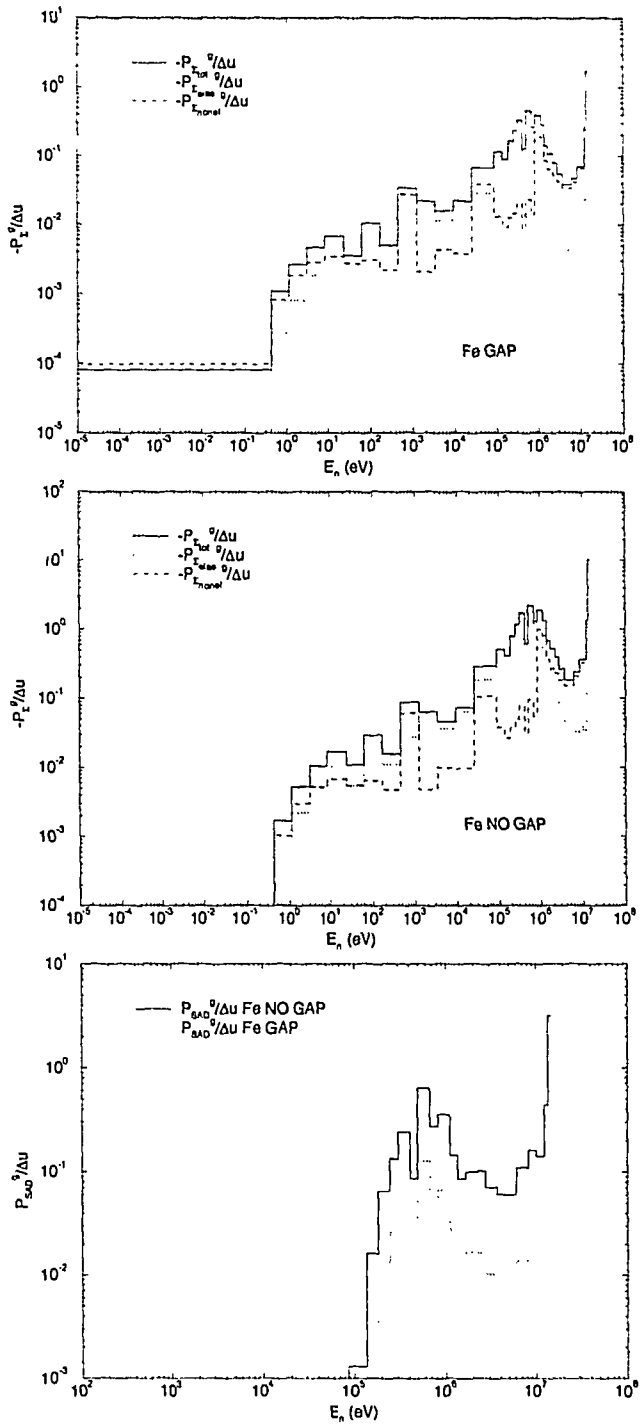

Figure 7: Sensitivity profiles for the total, elastic and non-elastic cross section of Fe for the gap-geometry (upper figure) and the no-gap-geometry (middle figure). In the lower figure the SAD-sensitivity profile for the $l = 1$ component of the elastic cross section of Fe is given. Response parameter: energy-integrated flux at the beginning of the vacuum vessel.

[6] A. Hogenbirk: *Sensitivity and Uncertainty Analysis of the nuclear heating in the coils of a fusion reactor*, Report ECN-C--90-034, Netherlands Energy Research Foundation ECN, August 1990

[7] K. Furuta, Y. Oka and S. Kondo: *A cross-section sensitivity and uncertainty analysis on fusion reactor blankets with SAD/SED effect*, Nucl. Eng. Des./Fus. 3 (1986) 287

[8] W. W. Engle Jr.: *A users manual for ANISN*, Report ORNL/K-1693, Oak Ridge National Laboratory, 1967

[9] R. D. O'Dell, F. W. Brinkley Jr., D. R. Marr and R. E. Alcouffe: *Revised User's Manual for ONEDANT: A Code Package for One-Dimensional, Diffusion-Accelerated, Neutral-Particle Transport*, Report LA-9184-M, Los Alamos National Laboratory, December 1989

[10] W. A. Rhoades and R. L. Childs: *The DORT Two-Dimensional Discrete Ordinates Transport Code*, Nucl. Sci. Eng. 99 (1988) 88, (RSIC code package CCC-484/DORT, March 1989)

[11] R. E. Alcouffe, F. W. Brinkley Jr., D. R. Marr and R. D. O'Dell: *User's Guide for TWODANT: A Code Package for Two-Dimensional, Diffusion-Accelerated, Neutral-Particle Transport*, Report LA-10049-M, Los Alamos National Laboratory, February 1990

[12] K. A. Verschuur and A. Hogenbirk: *Calculation of radiation fields inside and outside the NET cryostat/biological shield, Final report NET contract 89-226*, Report ECN-C--93-040, Netherlands Energy Research Foundation ECN, June 1993

[13] P. Vontobel and S. Pelloni: *JEF/EFF Based Nuclear Data Libraries*, EIR-Bericht Nr. 636, Eidgenössisches Institut für Reaktorforschung, 1987, updated version used (obtained in 1989)

[14] J. Stepanek: *TRAMIX: A Code for Interfacing MATXS Cross Section Libraries to Nuclear Transport Code for all Type Fission Reactor, Fusion Blanket as well as Shielding Analysis*, Paul Scherrer Institut (draft, 15-4-1988)

[15] J. F. Briesmeister (ed.), *MCNP - A General Monte Carlo Code for Neutron and Photon Transport*, Report LA-7396-M, Rev.2, Los Alamos National Laboratory, September 1986

[16] T. E. Booth: *A Sample Problem for Variance Reduction in MCNP*, Report LA-10363-MS, Los Alamos National Laboratory, October 1985

[17] P. Vontobel: *EFF1LIB: An NJOY Generated Neutron Data Library Based on EFF-1 for the Continuous Energy Monte Carlo Code MCNP*, PSI-Bericht Nr. 107, Paul Scherrer Institut, September 1991

[18] I. Kodeli and E. Sartori: *Covariance Data Library ZZ-VITAMIN-J/COVA*, Report for NEA Data Bank 1264 package, 1990, Revision 3